Geol. Soc. Malaysia, Bulletin 27, December 1990, pp. 27 – 55

Depositional environments, diagenesis, and porosity of reservoir sandstones in the Malong Field, offshore West Malaysia

NOOR AZIM IBRAHIM & MAZLAN MADON

Petroleum Research Institute, PETRONAS
Lot 1026, PKNS Industrial Area
54200 Ulu Kelang, Selangor

Abstract: The reservoir interval in the Malong Field, offshore West Malaysia, consists of three main types of sand bodies which are interpreted as a) prograding shoreface, b) shallow marine (inner-shelf), and c) fluvial channel sequences.

The prograding shoreface sequence consists of upward coarsening units in which heterolithic sandstone-mudstone are overlain by ripple cross-laminated and parallel-laminated sandstone. The inner-shelf sequence is made up of upward-coarsening offshore bar sandstones encased in shelf muds. The shelf sandbodies show evidence for deposition by storms, and are characterized by the association of distal, low-energy heterolithic facies overlain by proximal, amalgamated high-energy sandstone units. The fluvial channel sequence consists mainly of trough cross-bedded sandstone, intercalated with minor floodplain mudstone.

The Malong sandstones are buried at depths of not more than 150 m, and are probably in the early stages of diagenesis, as shown by the well-preserved depositional (primary) porosity. The porosity and permeability of the sandstones are related to depositional environments. Poroperm values are highest (ϕ = 25-36%, K = 100-800mD) in the channel and storm-deposited inner-shelf sandstones. Shoreface sandstones have slightly lower poroperm range (ϕ = 24-35%, K = 10-100mD), but are still considered as high-quality reservoirs. permeability barriers (ϕ = 10-22%, K<10mD) may be formed of lower shoreface and offshore mudstones.

INTRODUCTION

The Malong Field is located near the southwestern margin of the Malay Basin, offshore Peninsular Malaysia (Fig. 1). Two exploration wells, 5G-17.1 and 5G-17.2, were drilled on the western flanks of the Malong structure, and penetrated a lower Miocene alternating sandstone-shale sequence that rests on pre-Tertiary granitic basement. A sedimentological study was done to interpret the depositional environments, and examine the reservoir characteristics of the sandstones. This paper presents a summary of the results of the study.

GEOLOGICAL SETTING

The Malong Field is located on the Tenggol Arch, a basement horst block which separates the Malay and Penyu basins (Fig. 1). the basement is believed to be formed mainly of pre-Tertiary igneous and metamorphic rocks.

Presented at GSM Petroleum Geology Seminar 1988

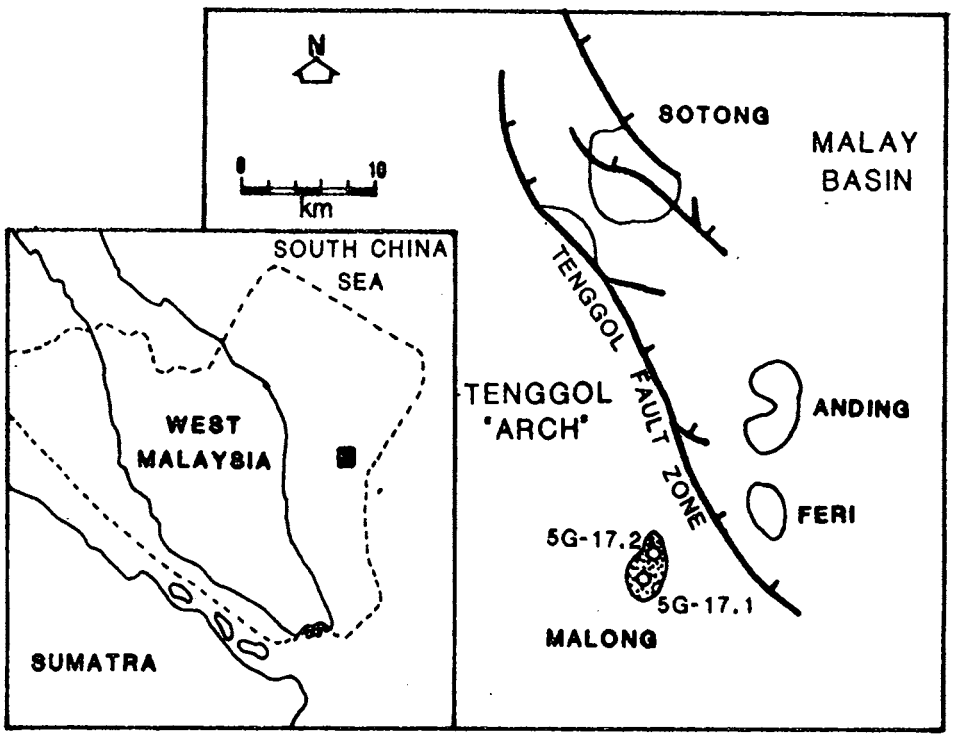

Figure 1: Location of Malong Field

The informal lithostratigraphy of the area is shown in Fig. 2. Nannofossils in the Tapis sandstone and basal Terengganu shale suggest a lower Miocene age. The Tenggol Arch was emergent until late early Miocene, when the area was inundated during a widespread transgressive event (Mazlan, 1990), which resulted in the deposition of the Terengganu shale. Reservoir sandstones occur in the overlying sand formation, herein referred to as the "Malong sandstone" (Fig. 2). This paper describes the sedimentary facies, diagenesis, and porosity-permeability relationships of the Malong sandstone.

Detailed description of the cores from well 5G-17.2 was carried out to determine the sandstone facies types, and interpret depositional environment. Wireline logs were used to correlate between the two wells.

Petrographic and mineralogical analyses were carried out using optical microscopy of thin sections, scanning electron microscopy (SEM), and X-ray diffraction (XRD). Porosity and permeability data were obtained from core-plug measurements.

AGE	NANNOFOSSIL ZONES	TENGGOL ARCH INFORMAL STRATIGRAPHY CONOCO-CARIGALI	THIS STUDY (MALONG FIELD)
EARLY-MIDDLE MIOCENE		"SAND-COAL FORMATION"	"SAND-COAL FORMATION"
			MALONG SANDS
	?	TERENGGANU SHALE	TERENGGANU SHALE
	NN4		
	NN3	TAPIS SANDSTONE	TAPIS SANDSTONE
	?		

Figure 2: Informal lithostratigraphical subdivision of lower-middle Miocene strata in the Tenggol Arch area. The reservoir section in Malong Field occurs at the base a coal-bearing sand-shale sequence, informally named the "Sand-coal formation". In this study, the term 'Malong sandstone' is used for the reservoir interval.

DEPOSITIONAL ENVIRONMENTS AND FACIES

The reservoir interval comprises three associations of facies, which are interpreted (Figs. 3, 4):

1) Prograding shoreface sandstones - This type of sandbody consists of and upward-coarsening sequence beginning with mudstone (facies MS) and heterolithic sand-mud facies (HB), grading upward into ripple cross-laminated and parallel laminated sandstone facies (SC).

2) Shallow marine (inner-shelf) sandstone - This facies association consists of generally upward-coarsening sequence of , from bottom to top, mudstone (MS), heterolithic facies (HB) and/or bioturbated and laminated sandstone (SB/SL), overlain by cross-bedded glauconitic sandstone (SX).

3) Fluvial channel - This facies association is dominated by through and planar cross-bedded, subarkosic sandstone, (SK) with minor intercalations of dark mudstone. Core logs of these facies associations are shown in Fig. 5. The individual facies are shown in Figs. 6 and 7, and are described below.

Mudstone (MS)

This facies is composed of dark grey, laminated and lenticular-bedded mudstone with abundant thin sand layers (Fig. 6A). The facies is moderately bioturbated, with numerous horizontal burrows possibly *Planolites* (Fig. 6B).

Sideritic layers and concretions are common. Glauconite and pyrite occur as accessory minerals, The facies may grade into the heterolithic facies (HB) as the sand content increases.

Facies MS is interpreted as offshore shelf mud deposit with intercalated distal storm sand layers (cf. Johnson and Baldwin, 1986).

Ripple cross-laminated sandstone (SC).

This facies consists of fine-to medium-grained, well sorted sandstone. Glauconite and sideritic mudclasts are present in small amounts. Sedimentary structures include small-scale, wave and current ripple cross-lamination, and horizontal lamination (Fig. 6E). Bioturbation is rare.

This facies represents deposition in middle-upper shoreface environment as shown by the dominance of parallel lamination, ripple cross-lamination, and its relationship with the other facies.

Bioturbated sandstone (SB)

This sandstones facies consists of highly bioturbated, argillaceous, very fine-grained sandstone (Fig. 7A). The sandstone is greenish grey, and contains abundant carbonaceous material, glauconite, pyrite and siderite.

This facies is interpreted to have been deposited in a low-energy lower shoreface to offshore environment, in which intense biogenic reworking has obliterated the physical sedimentary structures. The high percentage of matrix indicates poor winnowing in a low-energy setting. Similar facies has been described from recent lower shoreface to offshore transition settings (Rieneck and Singh 1973, Noor Azim, 1986).

Parallel laminated sandstone (SL)

This facies is composed of dominantly thinly parallel laminated, very fine-grained sandstone. Glauconite is present in this facies. Some of the finely laminated units display features which resemble hummocky cross-stratification

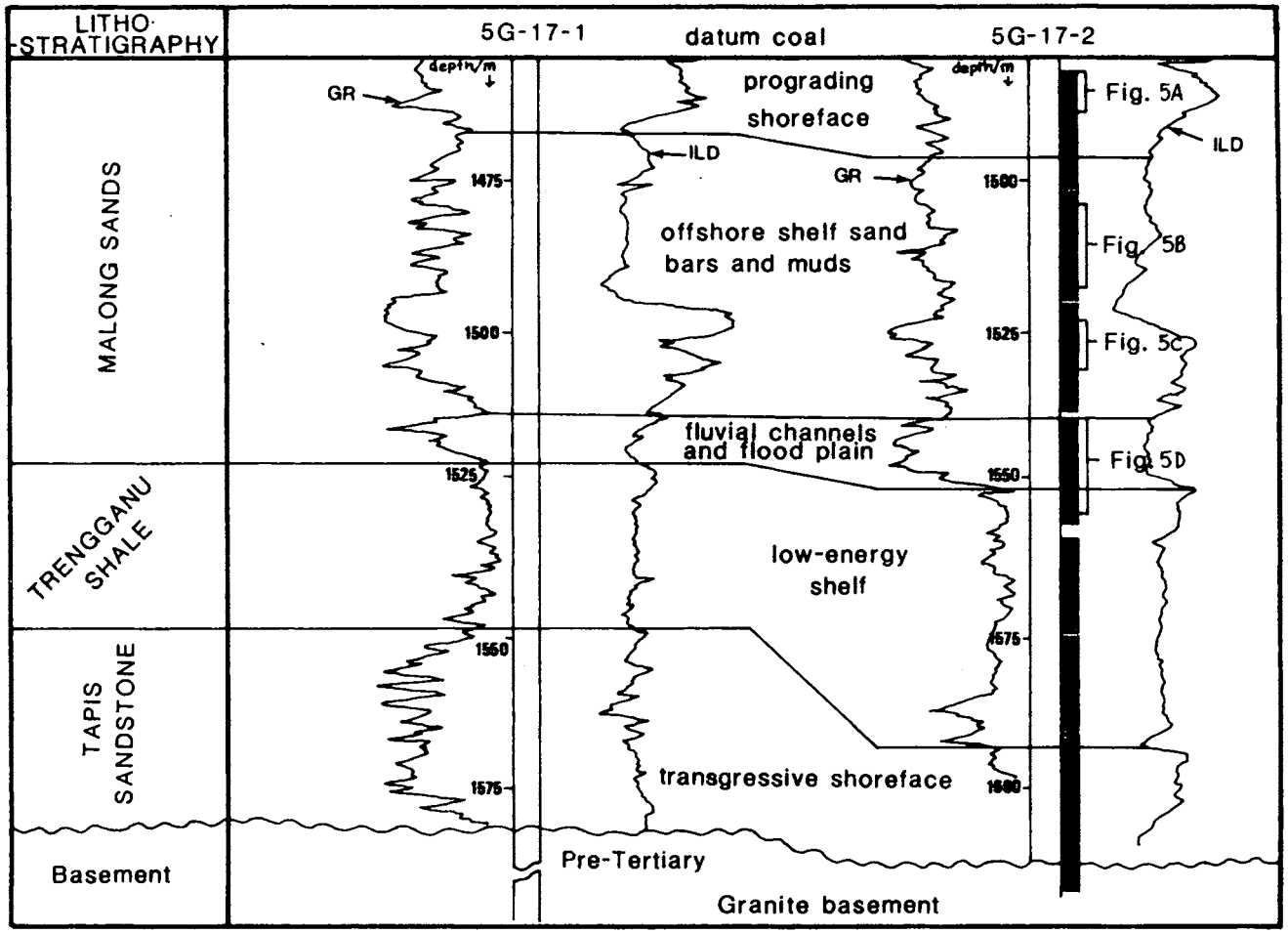

Figure 3: Cross-section through the two Malong wells showing the major depositional sequences. Representative sections of the core interval (shown in solid black) are presented in Fig. 5.

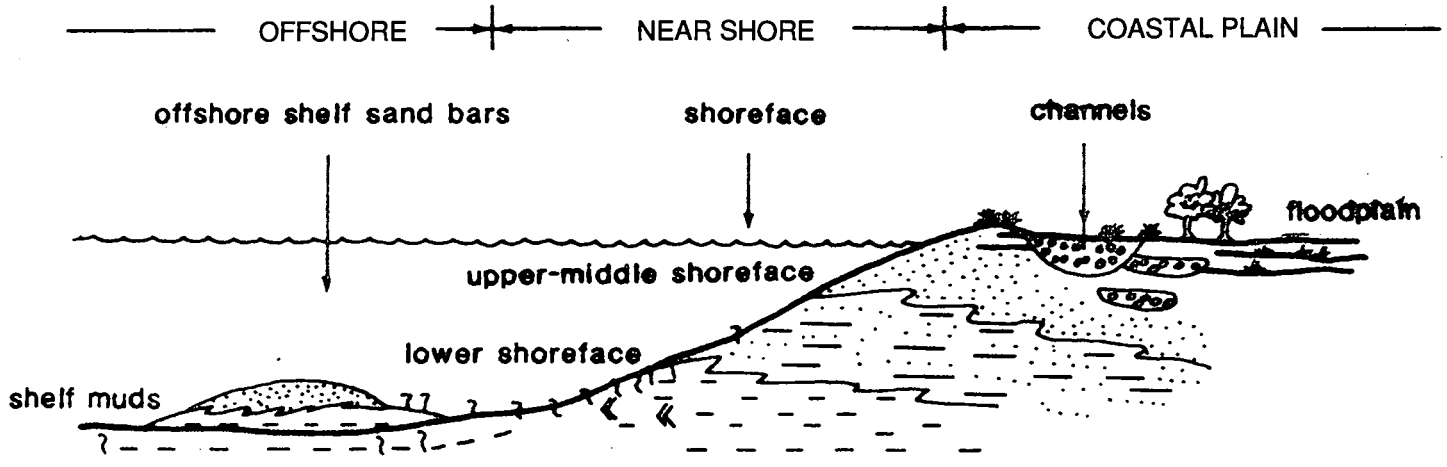

Figure 4: Schematic representation of the depositional environments for the Malong sandstone, as discussed in the text.

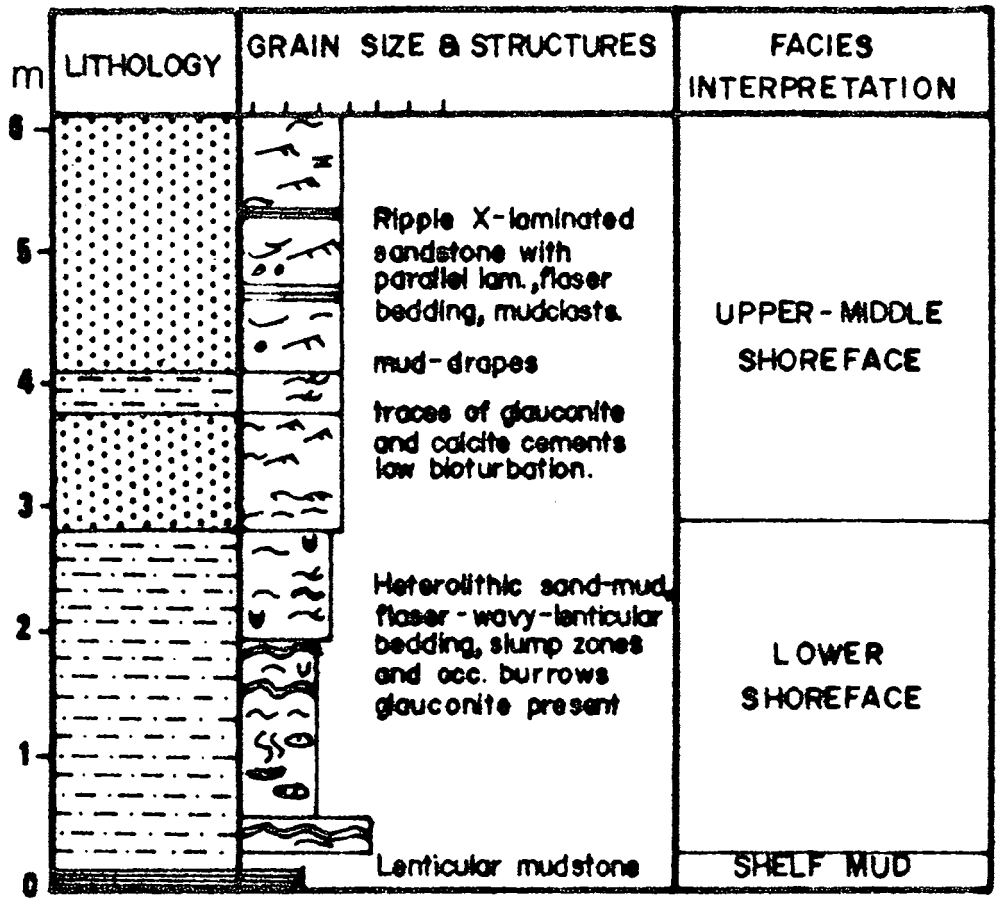

Figure 5A: Prograding shoreface sequence

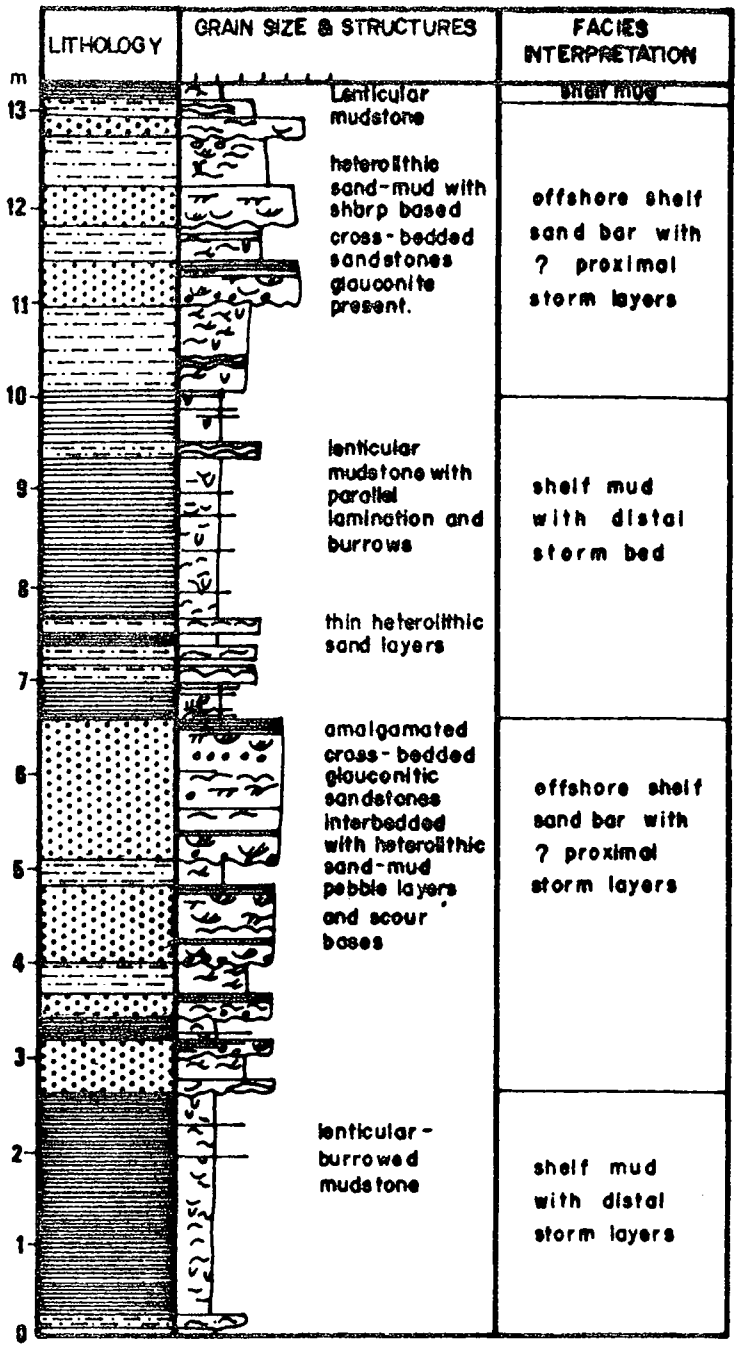

Figure 5B: Offshore shelf sequence

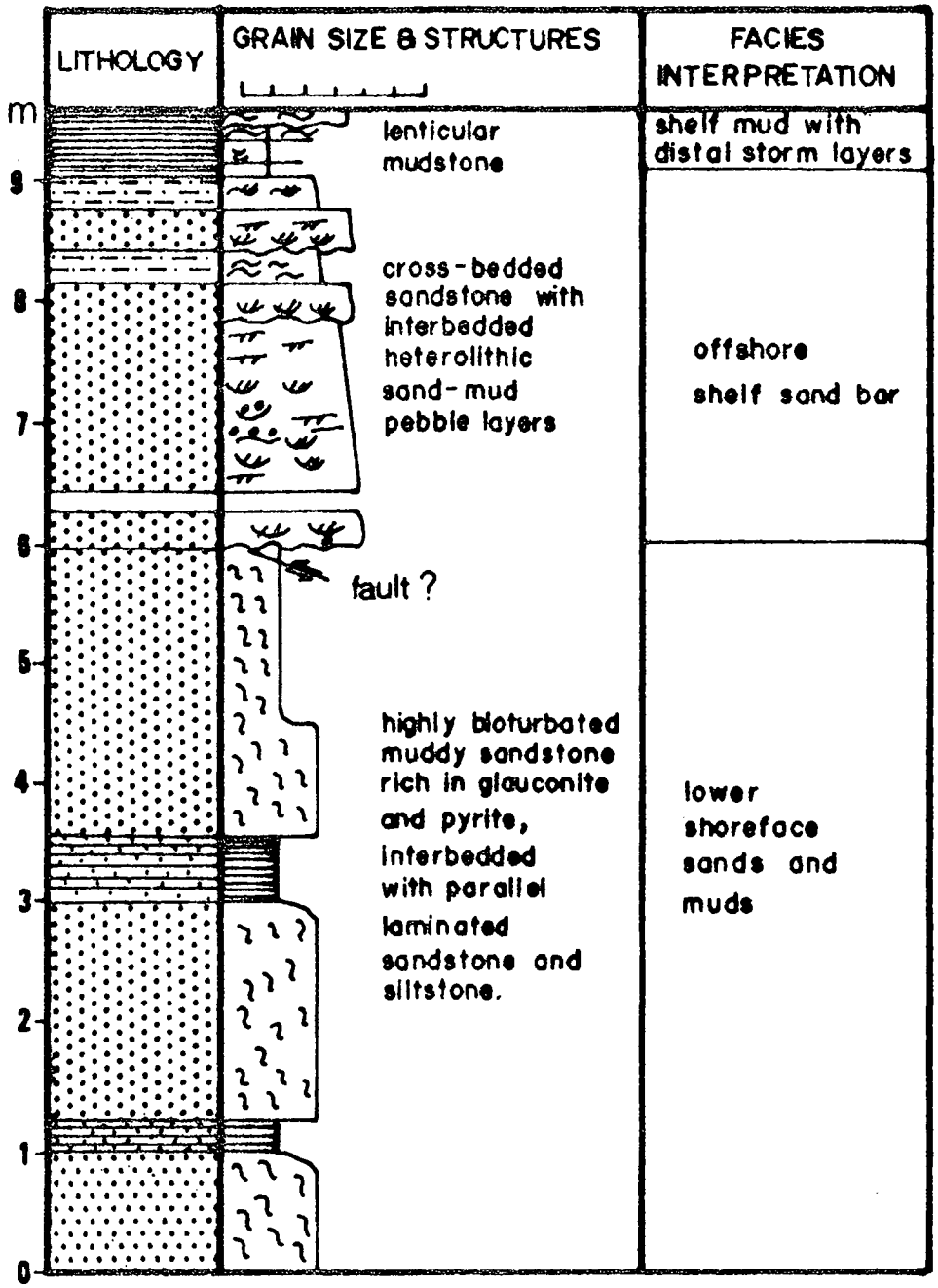

Figure 5C: Lower shoreface to offshore shelf sequence

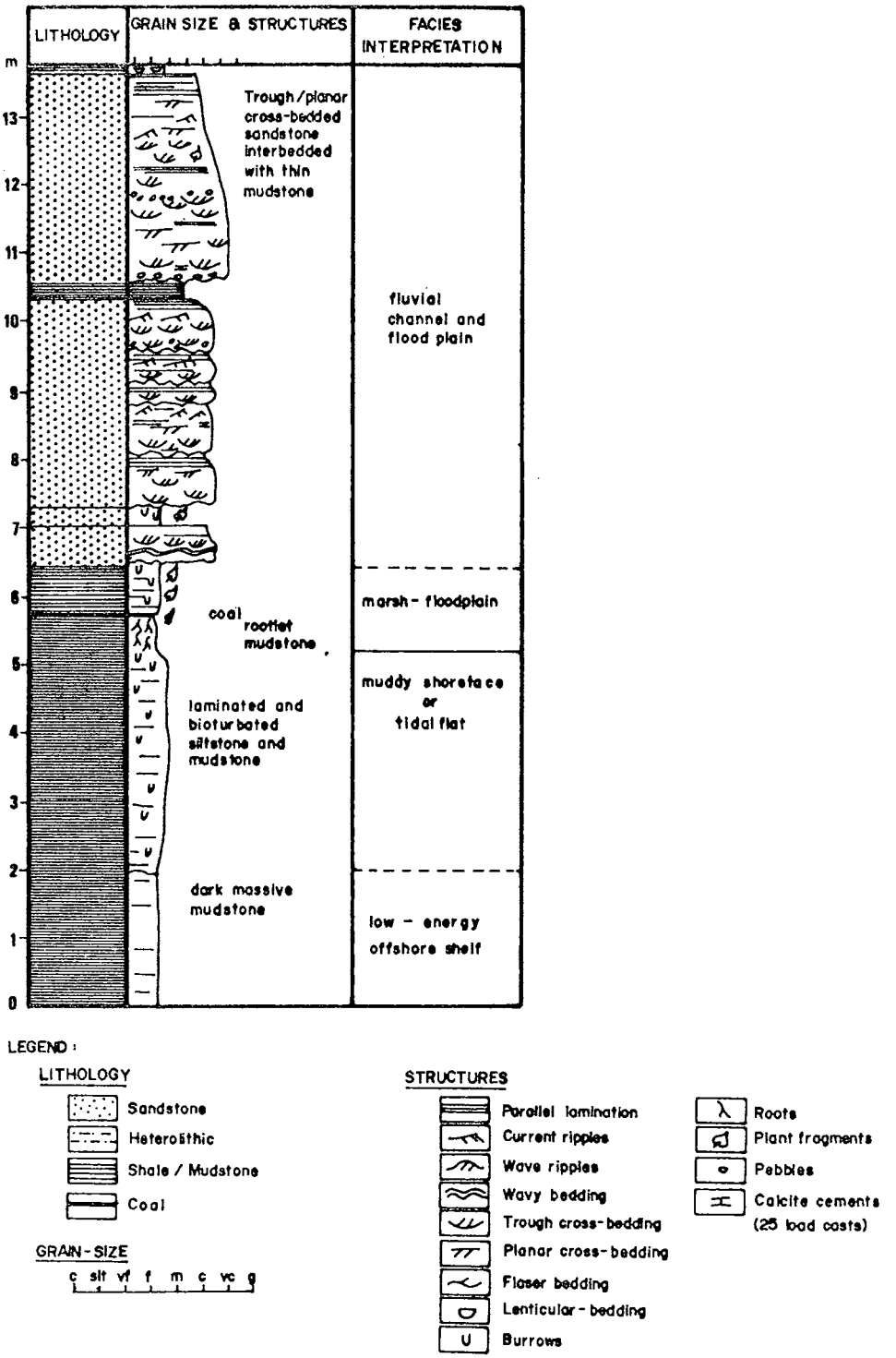

Figure 5D: Channel sequence

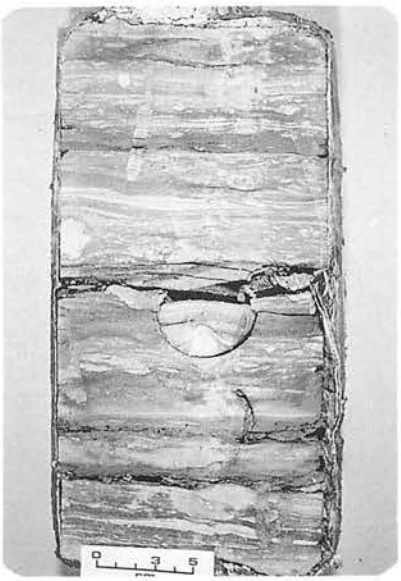

Figure 6A: Laminated, lenticular bedded mudstone (facies MS), with vertical and horizontal burrows.

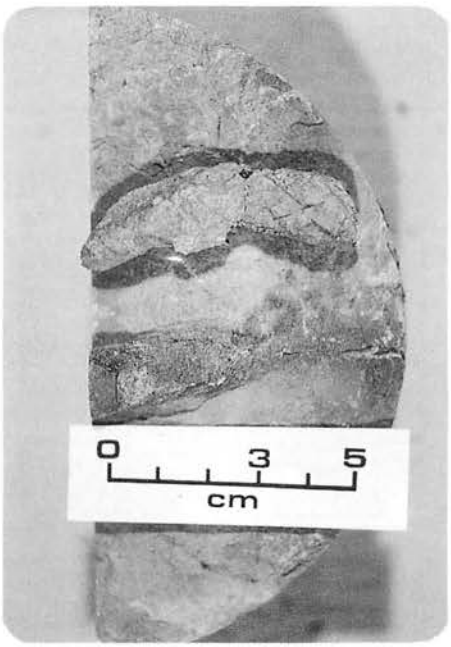

Figure 6B: Horizontal burrows possibly of *Planolites* in mudstone (Facies MS)

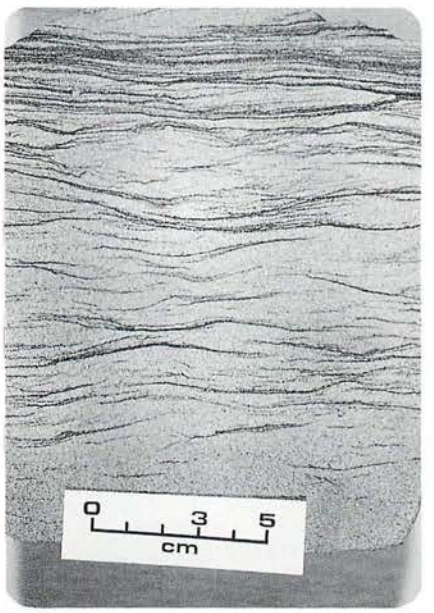

Figure 6C: Sand-rich heterolithic facies (HB) with flaser to wavy bedding formed by near-symmetrical wave ripples draped by mud.

Figure 6D: More muddy heterolithic facies (Hb) showing thinner sand layers and starved ripples, approaching the lenticular bedding typical of facies MS. Occasional burrows may be present.

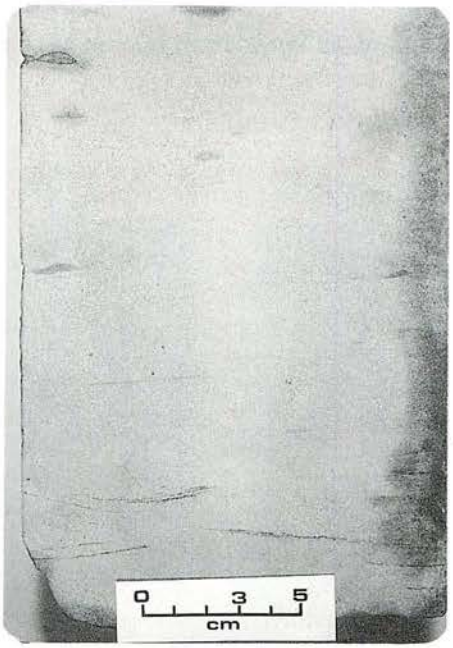

Figure 6E: Parallel laminated and ripple cross-laminated fine-grained sandstone (facies SC) interpreted as middle-upper shoreface sand.

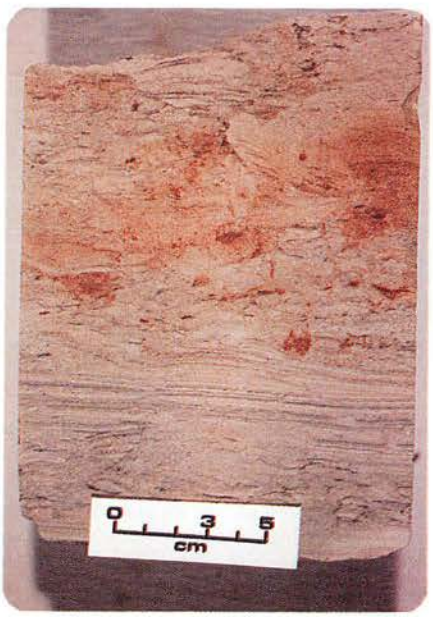

Figure 7A: Alternating bioturbated and parallel laminated sandstone (SB/SL) representing fairweather and storm conditions respectively.

(Fig. 7B). In places, the parallel lamination is seen to truncate the underlying bioturbated sandstone (SB).

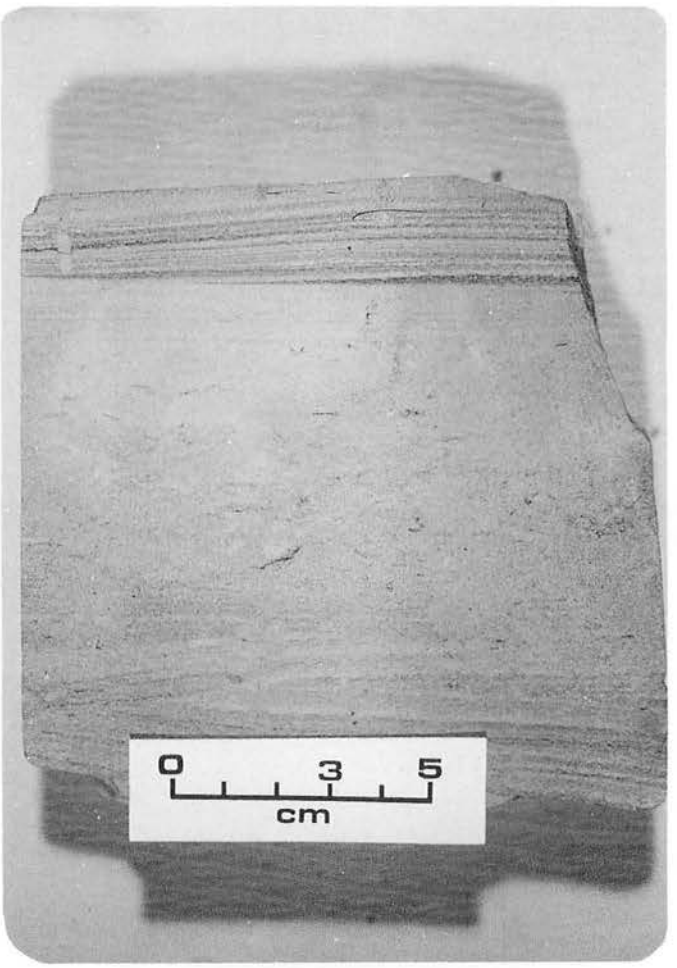

Figure 7B: Low-angle lamination (? possible hummocky cross-stratification - HCS) alternating with bioturbated units. The gradual contact between the laminated and the bioturbated units (bottom of picture) suggests that the latter was derived by biogenic reworking of]laminated sand during fairweather conditions. The laminated unit at the top presents another high-energy (storm) event, and forms a planar erosional surface with the underlying bioturbated sand. Note the lateral thickening of the parallel laminated sets, resembling HCS.

This facies is interbedded with the bioturbated sandstone (SB), which suggest that they are closely related. The alternation of laminated and bioturbated units, some with escape burrows, suggests episodic high and low energy (storm *vs* fairweather) conditions in the lower shoreface to offshore environment. The low-angle parallel lamination in facies SL is inferred to represent storm-generated structures known as hummocky cross-stratification (eg. Walker, 1979; Dott and Bourgeois, 1980).

Cross-bedded and low-angle bedded glauconitic sandstone (SX)

This facies consists of thickly bedded medium- to fine-grained glauconitic sandstones with scattered sideritic mudclasts. The main sedimentary structures are cross-bedding and horizontal to low-angle bedding. The cross-bedded sets are separated by thin sideritic mudstone layers (Fig. 7C, 7D). Mudclasts and carbonaceous material are common.

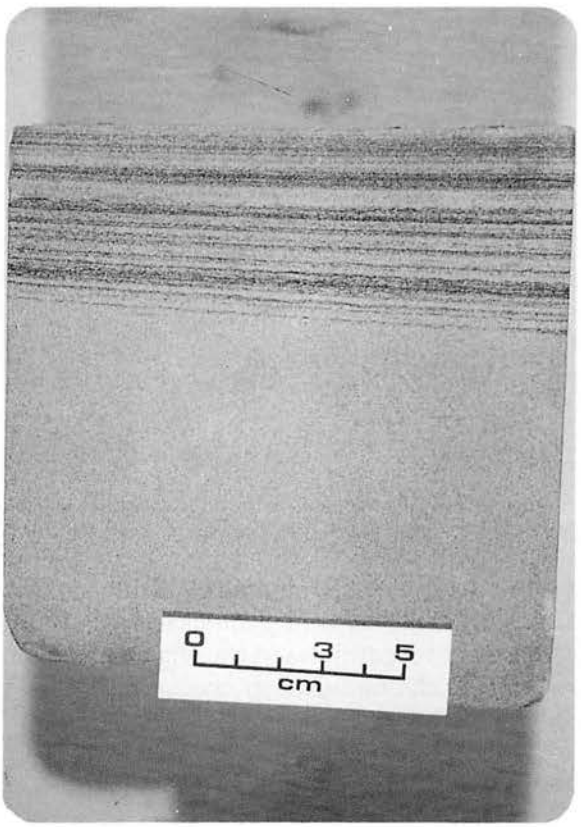

Figure 7C: Parallel lamination formed by organic-rich layers in thickly bedded sandstone (facies SX).

Figure 7D: Facies SX - Cross-bedded sandstone with sideritic mudclasts and organic material on the foresets. The bed is overlain by sideritic mud layer and thinly laminated sand.

This facies overlies the parallel laminated sandstone and bioturbated sandstone facies in the coarsening-upward sequence, and is interpreted as the product of migrating sandy megaripples in the offshore shelf environment. The facies probably represents the high-energy crestal part of offshore shelf sand bars (cf. Boyles and Scott, 1982).

Trough cross-bedded sandstone (SK).

This facies consists of medium to thickly bedded, medium to coarse-grained sandstone (Fig. 8A). The sandstone is slightly arkosic, and has a total thickness of 10 m.

Individual sandstone units are separated by 20 to 30 cm thick burrowed and lenticular bedded carbonaceous siltstone and mudstone. Basal erosional surfaces are overlain by coarse sand and granules. Trough cross-bedding at the base is succeeded upwards by parallel lamination and small-scale current ripple cross-lamination. Calcite concretions are present in the sandstones (Fig. 8B).

This facies is interpreted as a fluvial channel sequence based on i) the dominance of large-scale trough cross-stratification, ii) the numerous scour bases, and iii) the overall upward-fining trend. The calcite concretions, sometimes associated with plant roots, are probably calcrete features formed by soil-forming processes (Allen and Wright, 1988). Soil horizons with rootlets are also present in the underlying floodplain sediments.

Figure 8A: Trough cross-bedded, coarse-grained sandstone (SK).

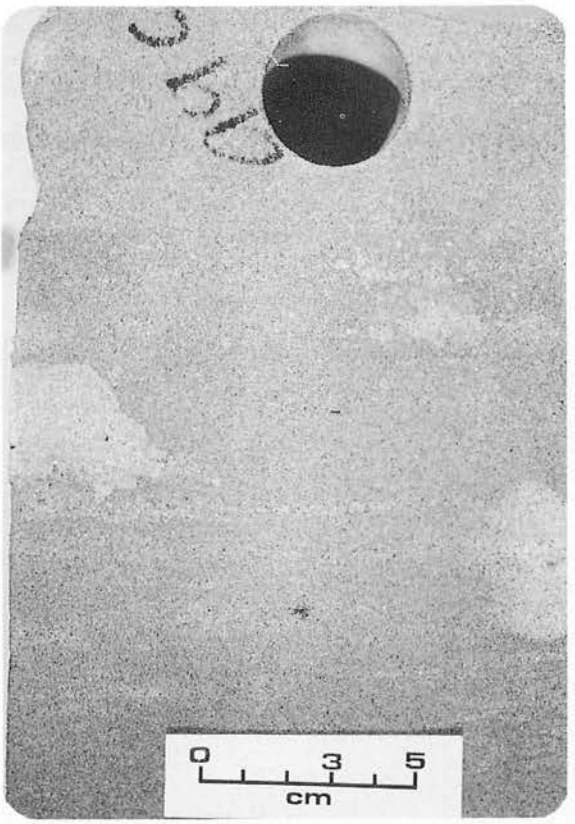

Figure 8B: Calcite concretions in facies SK.

PETROGRAPHY

The compositions of the sandstones were determined by point-counting 350 points per sample. Framework grain compositions are as follows : 42 to 52% quartz, 5 to 10% feldspar, and up to 9% rock fragments (Table 1). The sandstones are classified as lithic arkose, feldspathic arenite, subarkose and sublitharenite (Fig. 9).

Generally, the sandstones contain very little matrix. Detrital clay occurs as thin laminae, mud-drapes and mud-clasts. The percentage of detrital clay matrix in the coarser-grained sandstones may be up to 5% by volume, and is higher in the finer-grained sandstones. X-ray diffraction analysis of the clay faction (< 2μm) from sandstones showed that kaolinite constitutes more than 80% of the clay minerals, illite being the remainder. The well-crystalline morphology of the kaolinite (Fig. 12A) suggests that it is authigenic.

Table 1: Mineralogical compositions obtained from thin section point-counts (350 grains per slide). Q-detrital quartz, R-rock fragments, F-feldspar, MC-mica, CM-clay matrix, HM-heavy minerals, G-glauconite, q-quartz overgrowth, k-kaolinite/other clays, cc-clacite, s-siderite cb-carbonaceous material, p-porosity.

DEPTH/M	Q	R	F	MC	CM	HM	G	q	k	cc	s	cb	p	facies
1482.47	53.10	6.80	7.10	0.50	0.20	0.50			5.10		0.20		25.40	SC
1483.47	48.80	4.20	10.20	0.20	1.10		0.20		3.10	0.20	0.20		30.50	SC
1489.52	44.00	6.50	11.40		0.20	1.10		3.10	1.70		0.70		30.80	SC
1489.00	47.40	8.80	4.20	0.80		0.50		6.80					28.50	SC
1495.93	45.70	7.40	11.70	0.80	2.50	0.20		1.10	0.80				29.40	SX
1499.06	44.50	6.50	8.50	0.50	0.50	0.20		1.70	2.50				34.50	SL
1502.98	46.50	5.50	5.50		4.50	1.00	0.50			6.50			30.50	SX
1494.50	49.10	6.00	8.00	0.50				2.20	0.20		0.20		33.40	SX
1496.95	37.40	10.50	9.70	0.50	0.50			2.20	5.70				33.10	SX
1497.09	41.10	8.20	11.10		1.70			1.70	4.00		0.50		32.00	SX
1499.96	48.20	9.40	6.50	0.20	0.50	0.20		1.70	2.00				30.80	SX
1501.07	40.20	11.40	11.70	0.80	1.40			3.10	2.00		0.50		28.50	SL
1501.54	44.80	6.50	7.10		0.50	0.20		4.20	3.10		10.20		33.10	SL
1508.55	58.20	2.50	2.50				0.50	4.80	2.20		4.20		18.20	SX
1508.58	59.40	3.10	1.10				2.80	4.80	2.20		2.20		21.40	SX
1510.50	43.10	9.70	6.20				1.90	2.20	0.50		7.10		33.40	SX
1522.40	49.40	4.80	1.70	0.20	0.20		1.70	1.40					31.70	SX
1523.00	50.00	7.70	3.70		4.20		3.10	0.50	4.00				26.50	SX
1536.46	39.40	13.70	10.20	0.20	1.10			3.40	2.20				29.40	SK
1537.00	4.00	7.40	4.00	0.20	2.50	0.20		3.40	2.20			6.00	29.70	SK
1539.51	40.80	10.80	6.80	0.80		0.20		5.10	4.20		0.50		30.20	SK
1540.57	44.80	8.00	9.40	0.50	1.10	0.20		5.10	2.00				28.50	SK
1541.50	53.10	5.70	3.40					3.70	2.00				32.00	SK
1544.00	42.20	12.00	5.40					2.00	4.50				33.70	SK
1545.03	52.80	7.10	3.70	0.20				2.80	0.80				32.20	SK

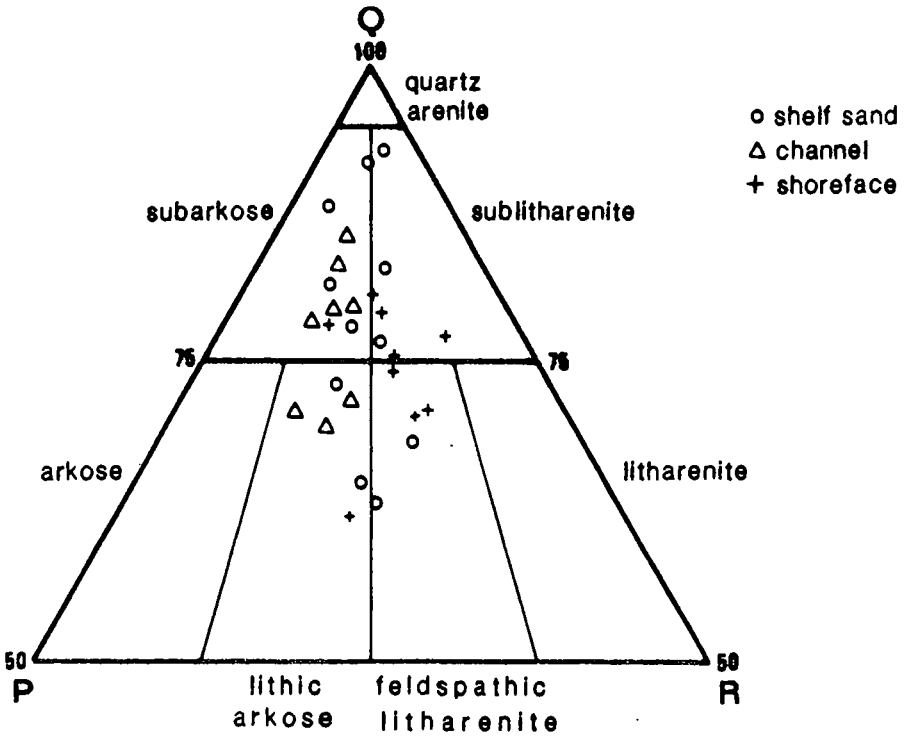

Figure 9: Framework grain composition of Malong sandstones, based on Folk's (1980) classification.

Authigenic minerals include quartz (2-7%), calcite (0.2%), siderite (0.2-10%), kaolinite (5%), and traces of pore-lining illite, chlorite and pyrite. Calcite cements are patchy and of limited distribution, and may totally fill the pore space of some sandstones (eg. facies SK). Pyrite is abundant as cement only of the bioturbated sandstone of the lower shoreface-offshore shelf environment (facies sb, Fig. 10A). Glauconite is particularly abundant in the shallow marine sandstones (facies SX).

In all the sandstones studied, grain-to grain contacts are mainly tangential (point) or long. Some sandstones even show "floating grain" texture. This indicates that very little compaction has occurred.

DIAGENESIS

The Malong sandstones are probably still undergoing burial, and are presently at depths of only about 1500 m. Their texture and mineralogy suggests that they have not reached an advanced stage of diagenesis. Features of deep burial diagenesis (depth >2-3 km) such as extensive pressure solution, quartz cemen-

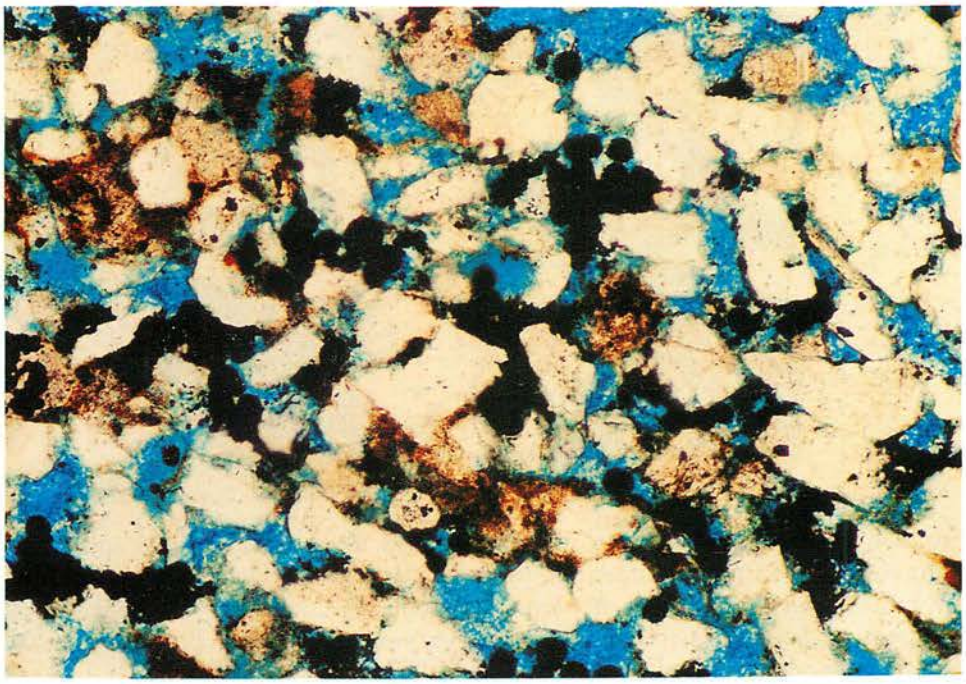

Figure 10A: Framboidal pyrite cements (black spots) in bioturbated sandstone (facies SB).

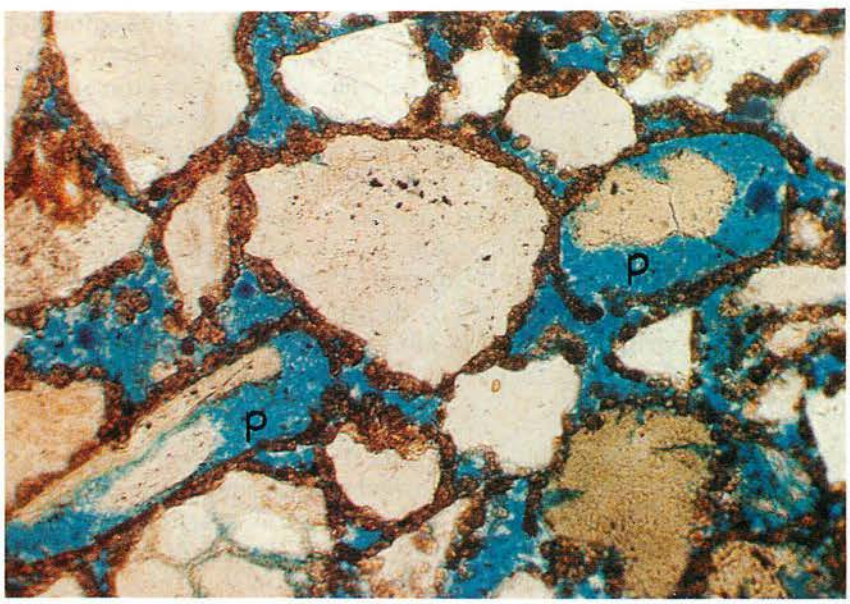

Figure 10B: Early diagenetic grain-coating siderite in glauconitic sandstone (facies SX). Some of the glauconite grains have been leached, creating secondary porosity (p).

Figure 10C: Poikilotopic ferroan calcite cement in channel sandstone (facies SK, cf. Fig. 8B).

tation, or illitization of kaolinite are not observed. Mechanical compaction seems to have been minimal as indicated by the texture and grain contacts, but may have been the main cause of porosity reduction during early burial. Many sandstones therefore still have porosities exceeding 30%. The present porosity is largely depositional (primary) intergranular porosity.

Most of the diagenetic features (Figs. 10–13) are the result of processes which occurred during early diagenesis and shallow burial. Pyrite and siderite are early diagenetic minerals formed by the reaction of iron in the sediments with CO_2 derived from organic matter decomposition (Curtis, 1978). Pyrite is particularly abundant in the lower shoreface and offshore sediments (facies SB, MS), suggesting the importance of sulphate in seawater in the formation of pyrite (cf. Berner, 1984). Ferroan calcite cements and concretions occur in the upper shoreface and channel sandstones. The high minus-cement porosity in the sandstones strongly suggests that the cements are early diagenetic in origin. The dissolution of carbonate shell fragments in the shoreface sands may have provided the ions for calcite cementation. Caliche-type concretions in the channel sandstones probably formed by precipitation form CO_2-charged porewaters of meteoric origin (cf. Goudie, 1983 p. 144 - 115). The volume of these carbonate cements appears to be low and their distribution restricted by paleoenvironmental factors.

Extensive dissolution of feldspar grains resulted in some new (secondary) porosity in the sandstones (Fig. 11a). However, since the amount of feldspar in the sandstones is low (less than 10%), and only a small amount of this has been dissolved, the amount of secondary porosity created is not as high as it may seem. Dissolution of feldspar also resulted in the formation of authigenic kaolinite and quartz cement (Fig. 12a) so that there may be no significant net increase in porosity. The dissolution of feldspar grains was probably caused by flushing of meteoric water during early burial (Bjorlykke, 1983).

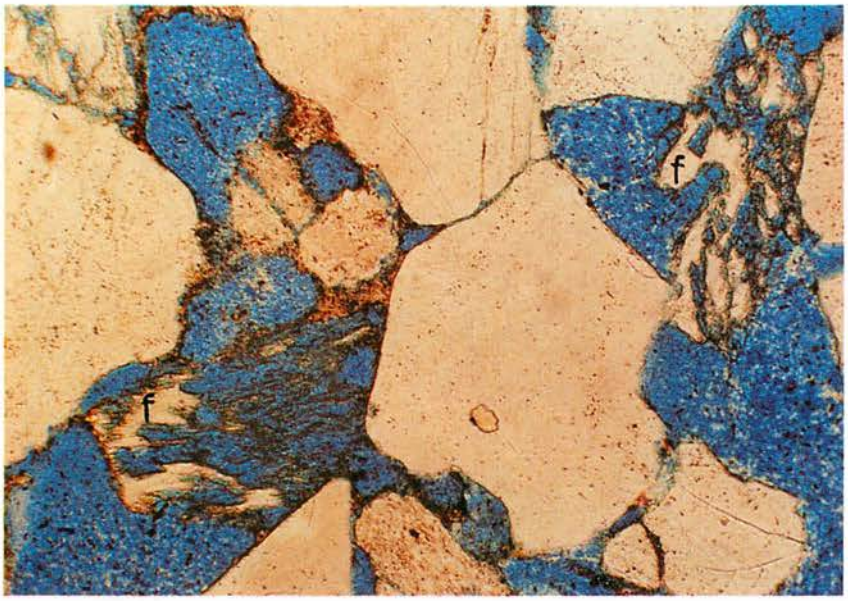

Figure 11A: Coarse-grained sandstone (facies SK) showing highly altered partially dissolved feldspar grains (f).

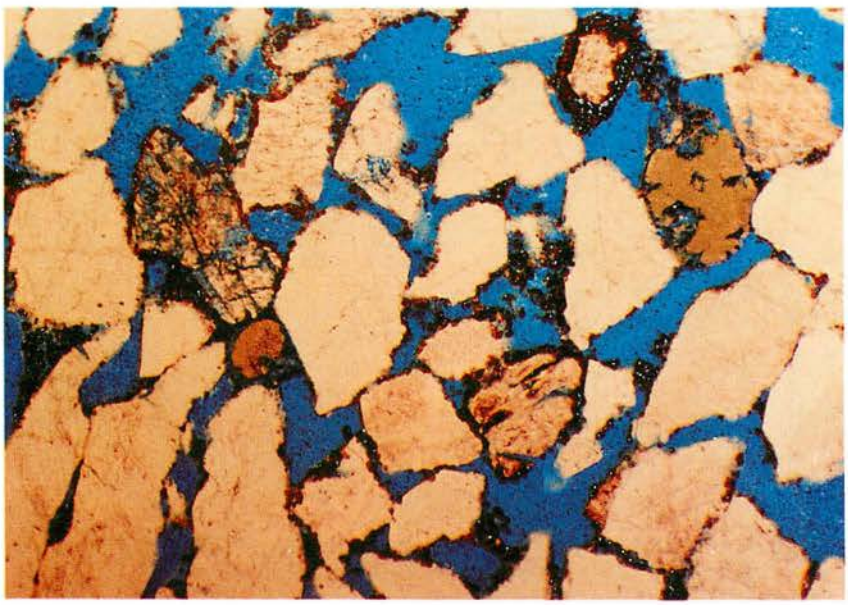

Figure 11B: The pore spaces in this picture (blues areas) is interpreted as mostly primary intergranular porosity. Sutured grain contacts are generally absent, suggesting low degree of compaction.

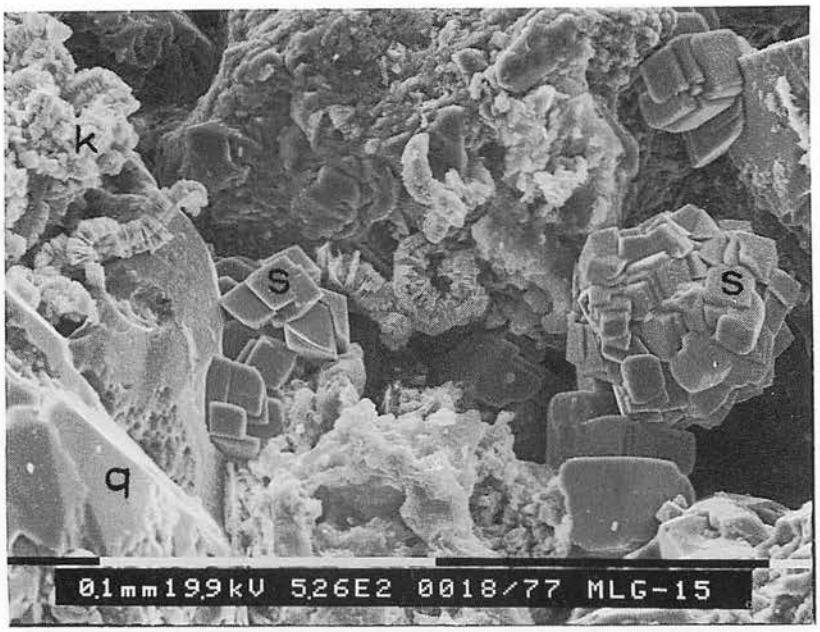

Figure 12A: Authigenic kaolinite (k), siderite (s) and quartz overgrowths (q).

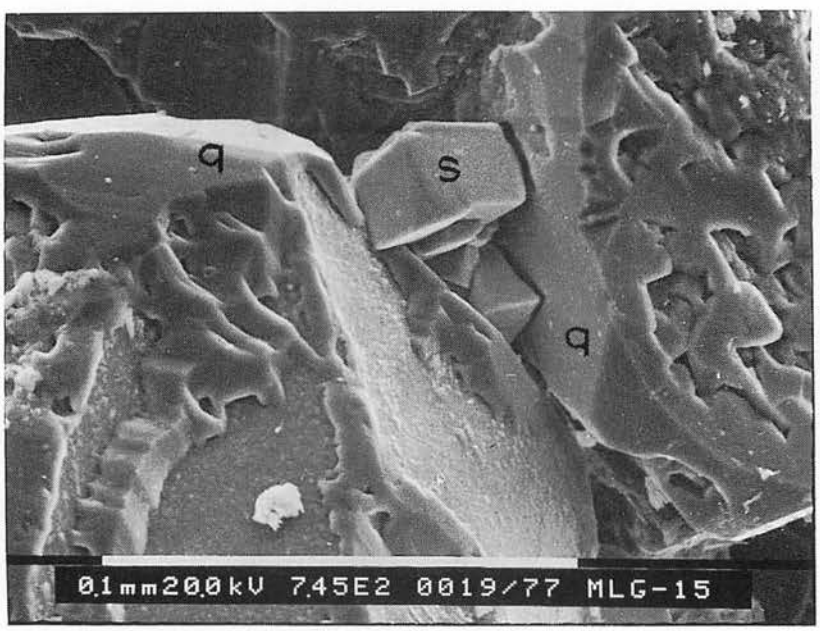

Figure 12B: Authigenic siderite crystals (s) and quartz overgrowths (q).

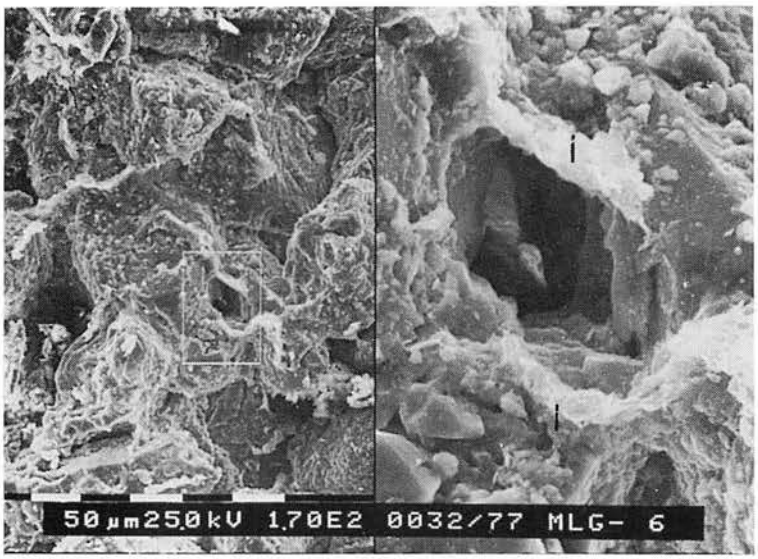

Figure 12C: Pore-lining illite (i) in sandstone (SX).

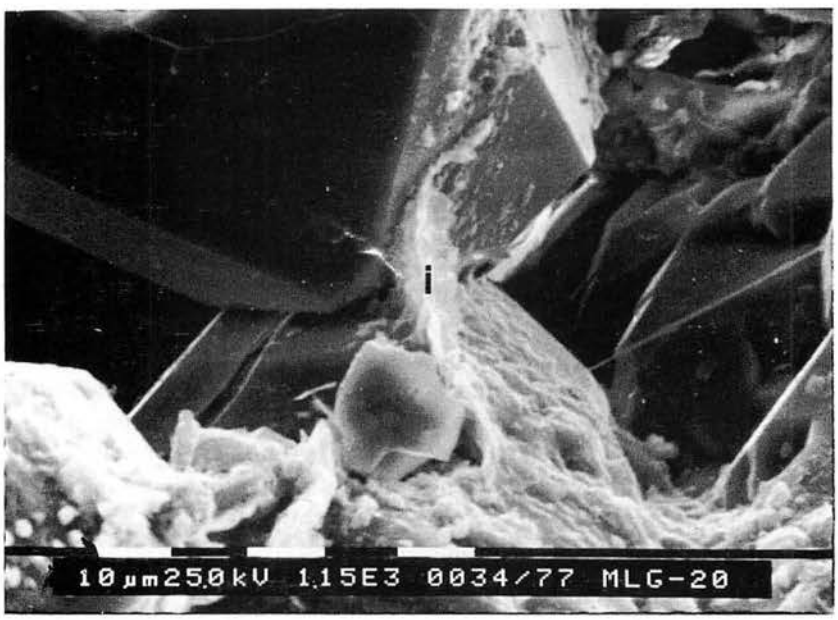

Figure 12D: Illite (i) post-dates quartz overgrowth (q) formation.

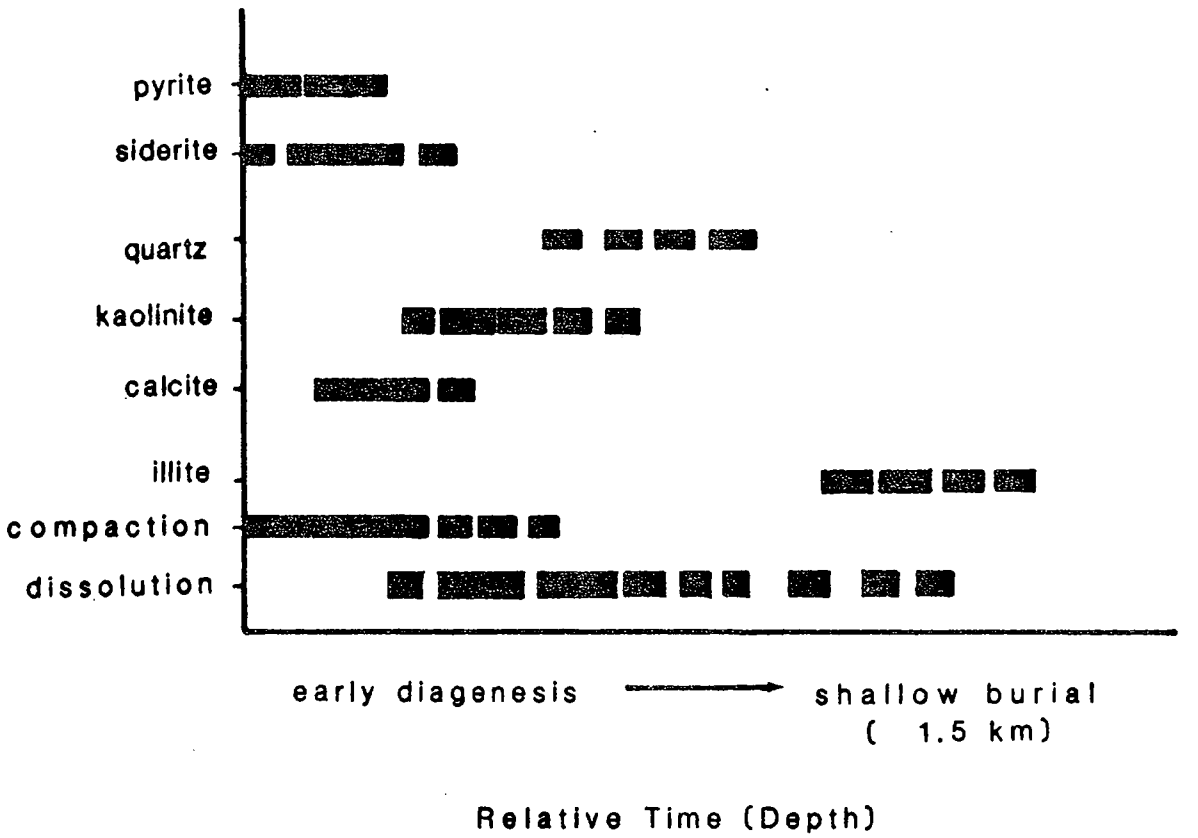

Figure 13: General sequence of diagenetic minerals in the Malong sandstones. See text for explanation.

As K- feldspar is dissolved, the concentration of K^+ ions in the pore water increases. Authigenic illite starts to precipitate when the pore-water reaches saturation with respect to illite at deeper burial conditions. Authigenic illite post-date quartz overgrowths, and occurs commonly as pore-lining material in the water-bearing sandstones (Fig. 12c). The illite is of flaky type, and appears to have formed partly by transformation of detrital mixed-layer clays. The very rare occurrence of illite in the hydrocarbon-bearing zones suggests that illite pricipitation may have been partly inhibited by the presence of hydrocarbons in the pore space, and that oil was emplaced into the reservoir slightly before or at the time of illite formation (Fig. 13). However, residual water saturation in the oil zones may have caused the formation of the traces of autihigenic illite in the oil zone (Ehrenberg and Nadeau, 1989).

POROSITY AND PERMEABILITY

The porosity and permeability of the sandstones are generally ralated to the type of facies (Fig. 14). The best reservoirs in terms of porosity and permeability, are of facies SX and SK which are the fluvial channel and offshore bar sequences (porosities 22-36%, permeabilities 100-800mD). shoreface sequences - facies SC, SL and HB (porosities 24-35%, permeabilities 10-1000mD). Slighty lower quality are formed of prograding. Bioturbated sadstones (facies SB) have poor reservoir properties due to high amounts of clay, pyrite and siderite. Permeability barriers which separate the sandbodies are formed of facies SB and MS (lower shoreface-offshore bioturbated sandstone and mudstone) which have porosities and permeabilities less than 22% and 10mD respectively.

CONCLUSIONS

The porosity and permeability of reservoir sandstones in the Malong field are primarily related to depositional environments (facies).

Poroperm values are highest (ϕ = 25-36%, K = 100-800mD) in fluvial channel and offshore shelf sandstones. Shoreface deposits have slightly lower poroperm values (ϕ = 24-35%, K = 10-1000mD).

The sandstones have only been buried at relatively shallow depths (<1500m) and very little cementation has taken place, and hence much of their primary porosity is preserved.

ACKNOWLEDGEMENTS

This paper is based on a project on the Malong Field undertaken for PETRONAS Carigali Sdn. Bhd. Nannofossils analyses by Awaluddin Harun. The paper is published with the permission from PETRONAS.

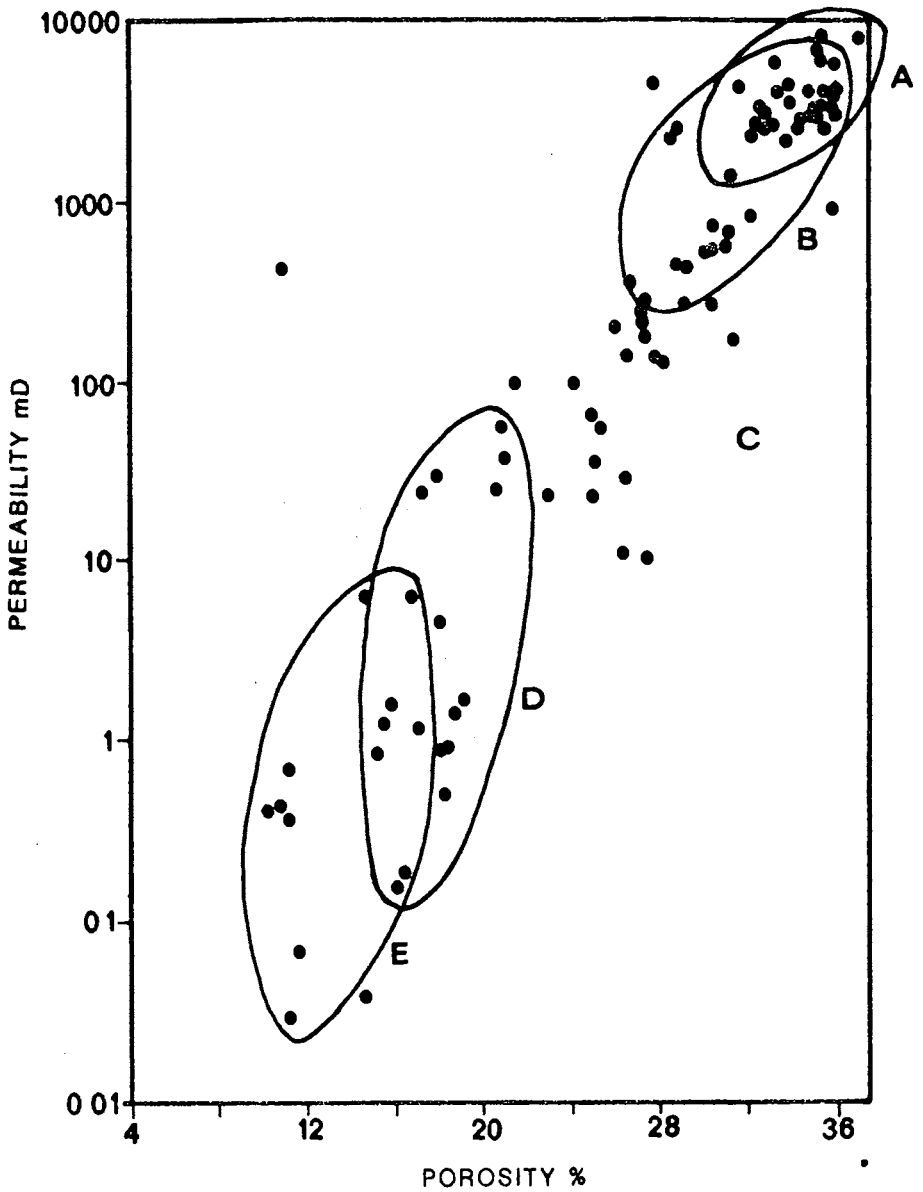

A – channel sandstones
B – offshore shelf sand bars
C – shoreface sandstones (middle-upper)
D – lower shoreface heterolithic sand-mud
E – lower shoreface bioturbated sandstones and shelf muds

Figure 14: Porosity-permeability cross-plot of the sandstones showing the general relationship between reservoir properties and facies.

REFERENCES

ALLEN,J. R. L. AND WRIGHT, V. P. 1988. *Paleosols in Siliciclastic Sequences*. PRIS Short Course Notes No. 001, Postgraduate Research Inst. for Sedimentology, Reading University, 98p.

ARMITAGE, J. H. and VIOTTI, C. 1977. Stratigraphic nomenclature–southern end Malay Basin. *Proc. Sixth Annual Conv, Indonesian Petroleum Assoc.* 1, 69-94.

BERNER, R. A. 1984. Sedimentary pyrite formation: an update. *Geochim. Cosmochim. Acta*, v. 48, p. 605-615.

BJORLYKKE, K. 1983. Diagenetic reactions in sandstone. *In* Parker, A. and Sellwood, B. W. (Eds.) *Sediment Diagenesis*, D. Reidel Publishing Co., 196-213.

BOYLES. J. M. and SCOTT, A. J. 1982. A model for migrating shelf-bar sandstones in Upper Mancos Shale (Campanian), northwestern Colorado. *Am. Assoc. Petrol. Geol. Bull.*, 66, 491-508.

CURTIS, C. D. 1978. Possible links between sandstone diagenesis and depth-related geochemical reactions occurring in enclosing mudstones. *J. Geol. Soc. London*, 135, 107-117.

DOTT, R.H. JR and Bourgeois, J. 1982. Hummocky stratification: significance of its variable bedding sequences. *Geol. Soc. Amer. Bull.*, 93, 663-680.

EHRENBERG, S.N. and NADEAU, P. H. 1989. Formation of diagenetic illite in sandstones of the Garn Formation, Haltenbanken area, mid-Norwegian continental shelf. *Clay Miner.*, 24, 233-253.

FOLD, R. L. 1980. *Petrology of Sedimentary Rocks*. Hemphill. Austin, Texas.

GOUDIE. A. S. 1983. Calcrete. *In* Goudie, A. S. and Pye, K.(Eds.) *"Chemical sediments and Geomorphology"*. Academic Press, London, 93-131.

JOHNSON, H. D. and BALDWIN, C. T. 1986. Shallow siliciclastic seas. *In* Reading, H. G. (Ed.) *Sedimentary Environments and Facies*. Blackwell, Oxford, 229-282.

MAZLAN MADON, 1990. Chamositic and phosphatic ooids in the Terengganu shale (lower Miocene), offshore Peninsular Malaysia. *Geol. Soc. Malaysia, Annual Geological Conference 1990*, Ipoh, 7-8 May 1990 (abstract).

NOOR AZIM IBRAHIM, 1986. *Sedimentological and morphological development of a coarse-grained barrier beach, Horseneck Beach, Massachussettes, USA*. Unpubl. Masters Thesis, Boston University.

REINECK, H.E. and SINGH, I. B. 1973. *Depositional Sedimentary Environments*. Springer-Verlag, New York.

WALKER, R. G. 1979. Shallow marine sands. *In* Walker, R. G. (Ed.) *"Facies Models"*. Geoscience Canada Reprint series no 1, 75-89.

Manuscript received 12th July 1990